18th Brazilian Congress of Thermal Sciences and Engineering
November 16-20, 2020 (Online)

ENC-2020-0663
THERMAL OXIDATIVE STABILITY OF JET FUELS IN HIGH REYNOLDS NUMBER FLOW

Guilherme Dias Martins
Jônatas Vicente
Mariana Tessmann Martins
Arthur Benedetti
Amir Antonio Martins Oliveira
Department of Mechanical Engineering, Federal University of Santa Catarina, Florianópolis, SC, CEP 88040-900, Brazil.
guilherme.martins@labcet.ufsc.br, jonatas.vicente@labcet.ufsc.br, marianatessmannm8@gmail.com,
arthur.bbbenedetti@gmail.com, amir.oliveira@gmail.com

Gerson Fernandes Araujo Junior
Mauro Iurk Rocha
Gerência de Tecnologia de Produtos, CENPES, Petrobras, RJ, Brazil.
gerson.araujo@petrobras.com.br, miurk@petrobras.com.br

Abstract. *In this work, the characteristic flow and heat transfer parameters of the JFTOT (ASTM D3241-20) and the HiReTS (ASTM D6811-02) methods for the assessment of the oxidative thermal stability of aviation kerosene are estimated. The original HiReTS equipment was retrofitted with new technologies. Then, two kerosene samples, one fresh and the other aged, are subjected to the HiReTS test with the objective of comparing different forms of calculating the HiReTS number under conditions of very high temperature oscillations. The results indicate that the JFTOT method subjects the fuel to a higher thermal stress mostly due to the longer residence time. However, the flow and heat transfer in the JFTOT test is affected by thermally developing conditions and buoyancy. The flow and heat transfer in the HiReTS test, on the other hand, occurs under a homogeneous, radially well stirred condition, making it into a more statistically predictable test. Comparing the methods of calculating the HiReTS number, the linear extrapolation method to calculate the HiReTS number is able to filter out temperature oscillations caused by measurement uncertainty and lack of proper temperature control and should be preferred over the standard method. Further testing is needed to determine the limit for the time interval for the linear extrapolation.*

Keywords: *thermal-oxidative degradation, aviation kerosene, sustainable jet fuels, green aviation.*

1 INTRODUCTION

The current designs of jet-propelled airplanes have to cope with higher demands for thrust and power generation, as part of the efforts to increase the energy efficiency of the aviation sector. As a result, modern jet engines operate under higher temperature and their mechanical and electronic components are subjected to higher thermal load. The engine thermal management system currently uses the fuel as a heat transfer fluid to remove heat from bearings, gear boxes, pumps, generators, drive and power converters (Langton et al., 2009, Bullock et al., 1998, Morris et al., 2006 and Huang et al., 2004). As the fuel is heated while flowing in contact with hot surfaces, it suffers thermal degradation, and may generate carbon deposits within the fuel and bounding surfaces (Kendall et al., 1987, Jankowski, 2010). The formation of solid deposits, not only degrades the effectiveness of heat exchange due to fouling (Hazlett, 1991), but also provokes obstruction of fuel nozzle orifices, turbine vanes and blades, ultimately changing the burner outlet temperature profile, causing loss of efficiency, and reducing the maintenance intervals (Sarnecki and Gawron, 2017). The relatively low temperature in which the thermal oxidation occurs (around 290 °C) combined with the high pressure of the fuel lines may significantly increase the fuel viscosity, causing flow restriction in heat exchangers, thus reducing the heat exchange effectiveness and compromising the engine operation (Beaver et al., 2009).

The thermal degradation depends strongly on the fuel composition, e.g., the degree of hydrogenation used to reduce the concentration of heteroatomic species from kerosene (Jia et al., 2020). The fuel thermal degradation occurs in the presence of dissolved oxygen, involving a free radical, autoxidation, chain mechanism (Heneghan and Zabarnick, 1994). The reactions lead to oxidation products (*e.g.*, alcohols, ketones and acids) which later form solid-phase precursors. The precursors coalesce in larger molecular-weight products, which become insoluble and finally precipitate (Beaver et al.,

2005). Figure 1 presents a diagram of the processes that lead to solid-phase formation during the fuel oxidative thermal degradation.

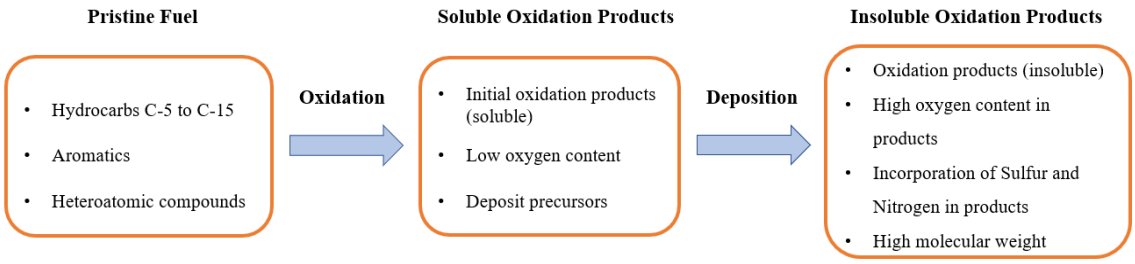

Figure 1. Formation of insoluble solid deposits from oxidative thermal degradation (adapted from Beaver et al., 2005).

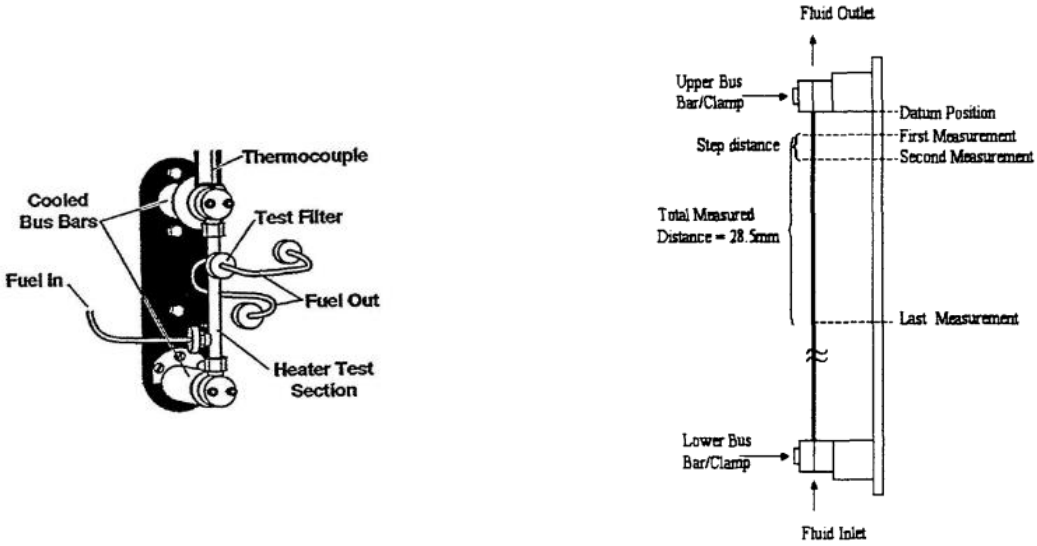

(a) Standard test section for JFTOT (ASTM D3241) (b) Test section for HiReTS

Figure 2. Test sections for the JFTOT and HiReTS tests.

The standard method to assess the thermal stability of jet fuels is the Jet Fuel Thermal Oxidation Tester (JFTOT) standardized as ASTM D3241-20. In this method, the fuel is pumped along an annular pipe under laminar flow and then through a standardized filter (Figure 2). The inner surface of the annulus is heated by Joule heating and the filter captures any insoluble deposits formed during the fuel degradation. Two observations are made from the test. First, the thermal degradation of the fuel forms a lacquer over the heated inner surface of the annular pipe and the color of this deposit is compared to a color scale. Secondly, the pressure drop through the filter caused by the capture of the solid residues from the fuel degradation is recorded. Both the color of the deposit and the pressure drop discriminate fuels of poor from acceptable thermal stability. The standard method has a drawback due to its qualitative nature, since the deposit at the tube wall is characterized by visual comparison to a color scale with five steps. Several works attempted to provide a more quantitative evaluation using optical reflectance, interferometry, ellipsometry and dielectric breakdown to measure the thickness and composition of the lacquer film. In an attempt to replace the visual evaluation of JFTOT tubes, ASTM has approved some interferometric and ellipsometric equipment manufactures and established a limiting thickness of 85 nm in an area of 2.5 mm² for the residue in JFTOT tubes for the jet fuel specification. But all these attempts to quantification overlook the facts that the flow in the test section is not one-dimensional and that the test method is no longer able to reproduce the fuel flow in modern jet engines (Sander et al., 2015).

Neageli (1997) and Pei et al. (2015) consider the formation of deposits as a two-step process. The first step is the oxidation of the fuel forming precursors and the second step is the mass diffusion of these precursors to the wall. Since the second step is strongly influenced by boundary layer transport, the Reynolds number and the energy boundary condition at the wall influence where the precursors are formed, their rate of coalescence and deposition at the wall. In most fuel lines in jet aircrafts, contrary to the conditions in the JFTOT test, the flow is turbulent. The High Reynolds Number Thermal Stability (HiReTS) test was envisioned to closely reproduce real fuel flow conditions. This method was created in the nineties through a partnership between the Universities of Sheffield and Leeds and Shell Global Solutions. It was identified as ASTM D6811-02, but it was later abandoned as an industry standard. In this method, the fuel is heated

in a circular capillary tube until it reaches 290 °C at the exit. The temperature at the external surface of the tube is recorded and the temperature increase in a 2-hour test provides a correspondent HiReTS number for the fuel.

Sanders et al. (2015) discusses that the extension of deposition on the JFTOT surface depends on the extension of the consumption of oxygen which depends on the residence time under temperature. However, the flow in the annular tube in the JFTOT is affected by buoyancy resulting in recirculation and a complicated distribution of residence time. The condition of turbulent flow and high heat flux studied by Jiang et al. (2013) showed that the consumption of oxygen depends on both temperature and residence time in a more predictable way.

The aim of this work is to analyze the flow and heat transfer conditions applied over the fuel during a standard test in the HiReTS method. These conditions are compared to the laminar conditions used in the JFTOT method and the differences of the two methods are discussed. A typical test was applied to fresh and aged samples of jet fuel and the differences in the results of the HiReTS method are also discussed.

2 MATERIALS AND METHODS

2.1 HiReTS experimental set-up and method

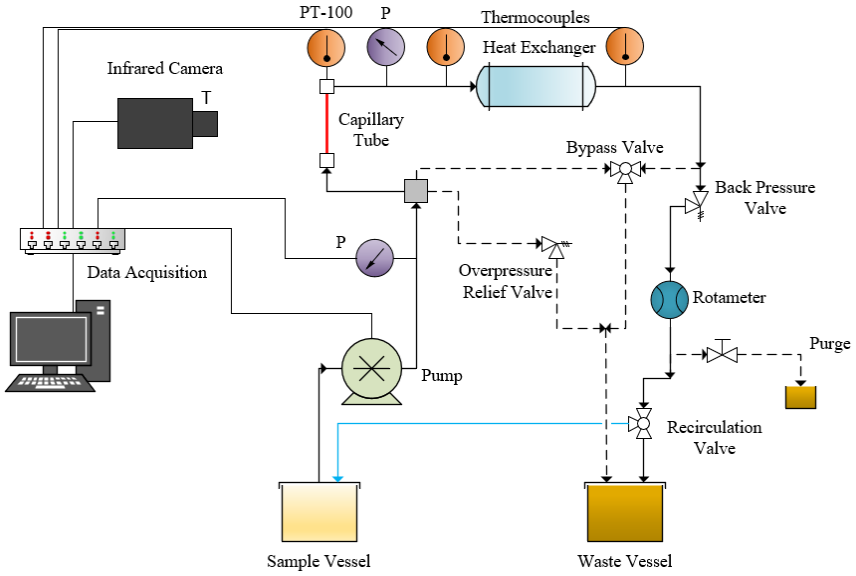

Figure 3. HiReTS experimental apparatus.

Figure 3 presents a schematic of the HiReTS experimental set-up developed in this work. The original HiReTS equipment was retrofitted with new technologies. The fuel is pumped from the sample vessel by an HPLC Knauer pump model AZURA Pump P 4.1S with flow rate range of 0.01 – 50 ml/min and maximum delivery pressure of 15000 kPa, to a 152 mm long 316 stainless-steel capillary tube with 0.26 mm inner diameter and 1.66 mm outer diameter. The capillary tube is connected to the positive and negative bornes of a power source is heated by Joule heating. The temperature of the fuel in the exit of the capillary tube is measured by a PT100 thermo-resistor. The power of the Joule heating is controlled to achieve a set-point temperature of 290 °C in the fuel flow at the outlet of the capillary tube. The volumetric flow rate is kept constant for 2 hours and the external temperature of the capillary tube is measured along time using a Flir Systems model A655SC infrared camera. After leaving the capillary tube, the fuel flows through a heat exchanger and then to a waste vessel. From the waste vessel, the degraded fuel may be disposed, or recirculated to the test section. The flow line also contains bypasses to prevent pressure buildup and uncontrolled temperature increase due to obstruction of the capillary tube. All piping, connections and valves, except the capillary tube, are made of 6 mm stainless-steel tubing from Swagelok. The data acquisition is done using a Keysight Agilent model 34972a data acquisition system.

The camera, the pump and all the sensors of temperature and pressure were integrated with the software LabVIEW. Following the standard method (Dufferwiel, 2011), the infrared camera was set to collect data in 9 points on the outer surface of the capillary tube. The first point is located at 1 mm away from the datum and 2.5 mm of space between one another. The camera has a resolution of 640 x 480 pixels with a minimum focal point distance of 200 mm, generating a reading area of 82 x 109 mm with pixel dimension of 0.17 x 0.17 mm. The camera uses a measurement technology based on 3 x 3 pixels to ensure a greater accuracy in the local measurement. The local temperatures were recorded in intervals of 15 s, 1 min, and 5 min (standard) during the 120 min of total test time. The pump was set to pump fuel at rate of 35 ml/min under initial pressure of 3.6 MPa. Once the test is finished, the data is downloaded in table form and the HiReTS number is calculated.

The standard form of calculating the HiReTS number is (Wilson et al., 2010):

$$\text{HiReTS Total Number} = \sum_{n=1}^{12} (\Delta T_{Final} - \Delta T_{Min}) \tag{1}$$

where ΔT_{Min} and ΔT_{Final} refer to temperature differences between the measured and the initial temperature for the test at each measured location ($1 \leq i \leq 12$). At each measured location, ΔT_{Final} is the last temperature recorded for that location at the end of the test and ΔT_{Min} is the smallest temperature difference recorded for that position, usually, at the beginning of the test. When the value registered by this index is above a certain threshold value, the fuel is said to be thermally unstable.

2.2 Analysis of JFTOT and HiReTS methods

Both methods are based on an indirect detection of thermal-degradation reactions followed by solid deposition in a reactive flow with non-uniform temperature distribution. The differences between both methods are the geometry of the test section and the flow regime.

2.2.1 JFTOT method

In this method, the fuel flows in the annular space of a concentric annular tube, driven by a pressure gradient. Naming r_i as the internal radius and r_o as the external radius of the annular section, the hydraulic diameter and Reynolds number are defined as

$$d_h = 2(r_o - r_i), \qquad Re = \frac{\rho\, d_h \langle u \rangle}{\mu}, \tag{2}$$

where μ is the fuel dynamic viscosity at the average flow temperature and $\langle u \rangle$ is the area-averaged flow velocity. In this method, the flow is laminar, the heating occurs at the inner wall, and the test section has length L.

Flow. The fully developed axial velocity profile under laminar flow, assuming newtonian, incompressible, constant properties fluid and neglecting buoyance effects, is (White, 2005)

$$u_z = \frac{1}{4\mu}\left(-\frac{dp}{dz}\right)\left[(r_o^2 - r^2) + \frac{ln\left(r/r_o\right)}{ln\left(r_o/r_i\right)}(r_o^2 - r_i^2)\right], r_i \leq r \leq r_o. \tag{3}$$

From this solution, the shear stress at the inner wall ($r = r_i$) is

$$\tau_w = \left(-\frac{dp}{dz}\right)\left[-\frac{r_i}{2} + \frac{(r_o^2 - r_i^2)}{4 r_i ln\left(r_o/r_i\right)}\right]. \tag{4}$$

The volumetric flow rate $\dot{V}$ is

$$\dot{V} = \langle u \rangle A_u = \frac{\pi}{8\mu}\left(-\frac{dp}{dz}\right)\left[(r_0^4 - r_i^4) - \frac{(r_o^2 - r_i^2)^2}{ln\left(r_o/r_i\right)}\right]. \tag{5}$$

where the flow area is $A_u = \pi(r_o^2 - r_i^2)$.

The Darcy friction factor is

$$f = \frac{64}{Re}\left[\frac{(r_o - r_i)^2}{(r_o + r_i)^2 - \frac{(r_o^2 - r_i^2)}{ln\left(r_o/r_i\right)}}\right]. \tag{6}$$

We note that when $r_i = 0$, $f = 64/Re$, as expected.

The hydrodynamic entry length may be estimated as $x_h/d_h \sim 0.05Re$.

Heat transfer. The heat transfer rate across the outer surface is neglected. The total heat transfer rate from the inner pipe wall to the fluid is

$$Q = q_{w,i}A_{w,i} = \rho\dot{V}c_p\left(T_{m,o} - T_{m,i}\right), \tag{7}$$

where $q_{w,i}$ is the heat flux at the inner surface, $A_{w,i} = 2\pi r_i L$, c_p is the average specific heat, $T_{m,o}$ and $T_{m,i}$ are the mixture averaged temperatures of the flow leaving and entering the test section.

The local Nusselt number at the inner wall is defined as

$$Nu_i = \frac{q_{w,i}\, d_h/\lambda}{T_{w,i} - T_m}, \tag{8}$$

where $T_{w,i}$ is the surface temperature at the inner surface and λ is the fluid thermal conductivity.

Neglecting axial conduction and viscous dissipation, assuming fully developed conditions and constant properties, the solution for the fluid temperature allows for calculating the local Nusselt number. From the values listed in Shah and London (1978), the following expression was curve fitted in the range $0.1 \leq (r_i/r_o) \leq 1$:

$$Nu_i = 4.540 + 0.8454\,(r_i/r_o)^{-1} - 0.01089(r_i/r_o)^{-2}, \qquad 0.1 \leq (r_i/r_o) \leq 1, \tag{9}$$

with correlation coefficient $R^2 = 0.999996$ and standard deviation $\sigma = 0.00607$.

The thermal entry length may be estimated as $x_h/d_h \sim 0.05RePr$.

Residence time. The laminar flow in the test section is a segregated flow. Neglecting buoyancy effects, the path lines are parallel to the pipe surfaces. Each fluid particle following a path line experiences a different residence time, given by the length of the test section and the velocity at the specific path line. In the absence of mass diffusion, the average residence time is that experienced by the particle flows at the average speed, $\bar{t} = L/\langle u\rangle$. The minimum residence time is the one experienced by the particle traveling in the path line where the maximum velocity occurs,

$$t_{min} = \frac{L}{u_{z,max}} = \left(\frac{L}{2\langle u\rangle}\right)\frac{1 + R^2 - 2R_m^2}{1 - R_m^2[1 - 2\ln R_m]}, \tag{10}$$

where the nondimensional position of the maximum axial velocity is

$$R_m = \left[\frac{1 - R^2}{2\ln(1/R)}\right]^{1/2}. \tag{11}$$

and $R = r_i/r_o$.

2.2.2 HiReTS method

In this method, the fuel flows within a circular tube, driven by a pressure gradient. Naming r_o as the external radius of the circular tube, the hydraulic diameter and Reynolds number are defined as

$$d_h = 2r_o\,, \qquad Re = \frac{\rho d_h\langle\bar{u}\rangle}{\mu}. \tag{12}$$

In this method, the flow is turbulent, the heating occurs at the outer wall, and the test section has length L.

Flow. The flow is tripped by its passage along different accessories in its way to the test section, therefore, it is possible to approximate it as a fully turbulent flow. Assuming that the tube surface is smooth, the Blasius correlation may be used to approximate the Darcy friction factor for the turbulent flow (Panton, 2013), as

$$f = \frac{0.3164}{Re^{0.25}}. \tag{13}$$

From the application of a balance of linear momentum, the shear stress at the wall may be written as (Panton, 2013)

$$\tau_w = \frac{1}{8} f\rho\langle\bar{u}\rangle^2. \tag{14}$$

Using the Blasius correlation, the shear stress at the wall becomes

$$\tau_w = 0.03326\rho\langle\bar{u}\rangle^{7/4}\nu^{1/4}{r_o}^{-1/4}\,, \tag{15}$$

where ν is the dynamic viscosity.

Blasius expression leads to the 1/7 exponent as an approximation for the time-averaged axial velocity profile, leading to the power-law velocity profile

$$\bar{u}_z = 1.2245\langle\bar{u}\rangle\left(1-\frac{r}{r_o}\right)^{1/7}. \tag{16}$$

The hydrodynamic entry length may be estimated as $x_h \sim 10 d_h$.

Heat transfer. The heating occurs across the outer surface. Therefore, the total heat transfer rate from the pipe wall to the fluid is

$$Q = q_w A_w = \rho\dot{V}c_p\left(T_{m,o} - T_{m,i}\right), \tag{17}$$

where q_w is the heat flux to the fluid at the outer surface and $A_w = 2\pi r_o L$.

Neglecting viscous dissipation and assuming fully developed conditions, the area-averaged Nusselt number may be obtained from Gnielinski correlation (Kays and Crawford, 1993),

$$Nu = \frac{(f/8)(Re-1000)Pr}{1+12.7(f/8)^{1/2}(Pr^{2/3}-1)}. \tag{18}$$

The thermal entry length may be estimated as $x_t \sim 10 d_h$.

Residence time. The turbulent flow tends to remove segregation. The average residence time is that experienced by the particle that flows at the average speed, $\bar{t} = L/\langle\bar{u}\rangle$. The minimum residence time is the one experienced by the particle traveling in the path line where the maximum velocity occurs,

$$t_{min} = \frac{L}{\bar{u}_{z,max}} = \frac{L}{1.2245\langle\bar{u}\rangle} \tag{19}$$

The viscous dissipation is not addressed in the equations above. However, a simple estimate of the temperature increase due to viscous dissipation, based on order of magnitude arguments, is

$$\Delta T_v \sim \frac{1}{\rho\dot{V}c_p}\frac{V\tau_w^2}{\mu} = \frac{\bar{t}}{\rho c_p}\frac{\tau_w^2}{\mu} \tag{20}$$

3 RESULTS AND DISCUSSION

In this section, first the two methods are compared and then a typical result from the HiReTS method is presented and discussed.

3.1 Comparison between the JFTOT and HiReTS methods

Table 1 presents the operation parameters for the JFTOT and HiReTS tests. For the estimates, the thermo-physical properties of aviation kerosene are approximated by those of n-dodecane. Table 2 presents the thermo-physical properties of n-dodecane evaluated at the axial fluid average temperatures for the JFTOT and HiReTS methods.

Table 3 presents the comparison between the estimated parameters of the JFTOT and HiReTS methods. From the estimates, considering that the flow is sufficiently tripped before entering the test section, the flow in the HiReTS method may be considered fully turbulent. For both methods, the hydrodynamic entry length is estimated as occurring within 2 % of the length of the test section, allowing to use the fully developed flow estimates. We note that the average shear stress at the tube wall for the HiReTS method is about 3×10^4 larger than in the JFTOT method. The higher shear rate at the wall may have an effect of enhancing the fluid degradation, but this is not confirmed in the literature yet. Simple order of magnitude concepts, leads to estimating the temperature increase due to viscous dissipation as 10^{-6} K for the JFTOT method and 3 K for the HiReTS method, therefore, not very expressive either way.

Table 1. Operation parameters for the JFTOT and HiReTS methods.

Parameter		JFTOT	HiReTS
Volumetric flow rate, $\dot{V}$	m³/s	5.00×10^{-8}	5.833×10^{-7}
Inlet temperature, $T_{m,i}$	K	298	298
Outlet temperature, $T_{m,o}$	K	533	563
Inner radius, r_i	m	0.00159	-
Outer radius, r_o	m	0.00248	0.000130
Hydraulic diameter, d_h	m	0.00178	0.000260
Heated length, L	m	0.06033	0.152
Heated surface area, A_w	m	6.02×10^{-4}	1.24×10^{-4}
Pressure, p	MPa	3.4	3.8
Test time, t_{test}	s	9000	7200

Table 2. Thermo-physical properties of n-dodecane ($C_{12}H_{26}$) (from NIST web site).

Thermo-physical properties		JFTOT	HiReTS
Density, ρ	kg/m³	657.5	644.6
Dynamic viscosity, μ	Pa.s	3.47×10^{-4}	3.04×10^{-4}
Kinematic viscosity, ν	m²/s	5.28×10^{-7}	4.72×10^{-7}
Thermal conductivity, λ	W/m-K	0.110	0.107
Specific heat, c_p	J/kg-K	2655	2720
Prandtl number, Pr	-	8.4	7.8

Table 3. Comparison of parameters of JFTOT and HiReTS tests.

Property		JFTOT	HiReTS
Flow:			
Average flow velocity, $\langle u \rangle$, $\langle \bar{u} \rangle$	m/s	0.0044	11
Reynolds number, Re	-	14.85	6051
Friction factor, f	-	0.405	0.0359
Wall shear stress, τ_w	N/m²	0.0113	348.9
Hydrodynamic entry length, x_h/L	-	0.02	0.02
Heat transfer:			
Heat transfer rate, Q	W	20.51	271.1
Wall heat flux, q	kW/m²	34.1	2183
Nusselt number, Nu	-	5.83	50.5
Surface Temperature at outlet, T	K	627	669
Temperature difference wall-fluid	K	94	106
Thermal entry length, x_t/L	-	0.18	0.02
Residence time:			
Average residence time, $\bar{t}$	s	13.7	0.014
Minimum residence time, t_{min}	s	9.1	0.011

The thermal entrance length for both methods is estimated as 18 % of the tube length for the JFTOT method and 2 % for the HiReTS method. Therefore, the JFTOT method is affected by thermally developing effects. The wall heat flux is about 64 times larger but the surface temperature, assuming fully developed flow at the end of the pipe, is only about 41

K higher for the HiReTS when compared to the JFTOT method. The higher surface temperature may promote a strong adherence of lacquers on the wall, but this also needs to be confirmed experimentally.

The largest difference exhibited by both methods is the residence time. The average residence time of the JFTOT method is almost 1000 times longer than the average residence time of the HiReTS method. However, while the flow in the HiReTS is weakly segregated, the flow in the JFTOT is strongly segregated and also affected by buoyancy. Sanders et al. (2015), using numerical simulation to calculate the exit age distribution function, estimated that the most probable residence time is about 5 s, but there is a second peak at 21 s. The lower residence time is due to the contraction of the primary flow caused by a large recirculating secondary flow created by buoyancy. This shows the complexity of the laminar flow within the test section of the JFTOT, a feature that is not desirable in a standard test.

In summary, it is our conclusion that the JFTOT test subjects the fuel to a higher thermal stress than the HiReTS test, mostly due to the very long residence time under heating. However, this method has the drawback of having a complicated flow, affected by buoyancy and thermally developing conditions. The HiReTS method has a much simpler flow, a basically homogeneous turbulent flow, which tend to be statistically reproducible. Also, the evolution of the kinetics of degradation and deposition in the fuel would find a transport limited segregated flow in the JFTOT test section, while it would occur under a basically homogeneous flow in the HiReTS method, turning it into a more statistically predictable test.

3.2 Analysis of the estimation of the HiReTS total number

In the following, the results of two typical tests in the HiReTS set up are presented. Alternatives to the standard method for calculation the HiReTS number are presented and discussed.

3.2.1 Fresh Sample

Figure 4 presents the temperature measured in the external surface of the test section using the IR camera. The position axis indicates the coordinate measured from the outlet of the test section. The time axis indicates the test time. The temperature axis indicates the difference from the measured to the initial temperature. The oscillations observed in the temperature response are due to an inadequate setting of the temperature control. During the test, the fluid temperature at the outlet of the test section is kept constant. Solid deposition on the internal surface of the test section causes fouling resulting in an increase in the radial thermal resistance. Since the heat is generated within the pipe wall, by Joule heating, the increase in the thermal resistance for the heat transfer to the flowing fluid causes the increase in the wall temperature, which is captured by the measurement with the infrared camera. The color scale at the right indicates that the maximum temperature increase during the test was 23.3 C. The behavior depicted in this figure is typical of a fuel sample exhibiting very small degradation during the test time.

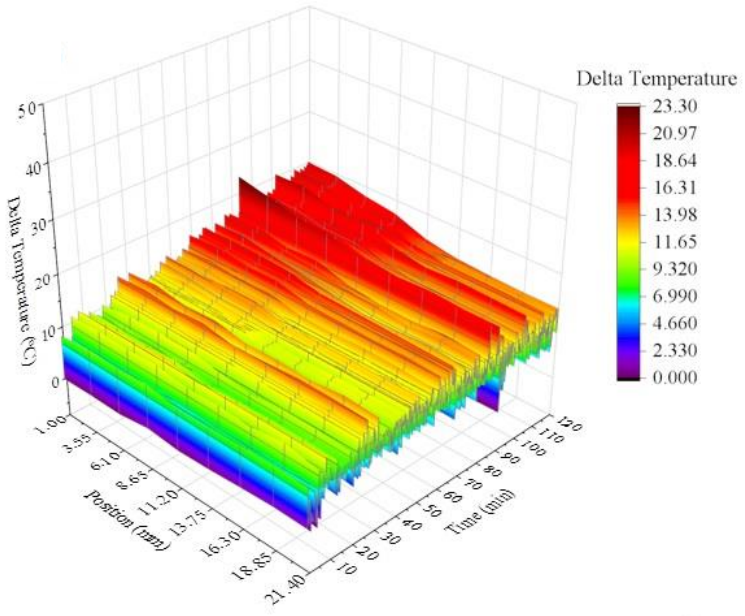

Figure 4. Temperature measured at the surface of the test section by the infrared camera during the HiReTS test of a fresh fuel sample. The temperatures are displayed with a 15 seconds data acquisition interval.

Table 4 presents the HiReTS Number calculated for this experiment. The standard method records temperatures with 5 min intervals and uses the last temperature to evaluate ΔT_{Final}, as described in Equation (1). The standard method provided a HiReTS total number of 61. This is a very low HiReTS number, indicative of a very thermally stable fuel. However, the specific value of the final temperature used in the standard method is affected by temperature oscillations caused by the control system, as shown in Figure 4. Therefore, in order to assess the effect of control oscillations in the test results, other strategies where also used for computing the HiReTS number. First, the time interval between the values of temperature actually used for the calculation of the HiReTS number was reduced to 1 min and then to 15s (the data are from the same experiment). Then, the final temperature was estimated from an extrapolation of a linear curve fitting using the measurements recorded at the time interval indicated. We observe that, as the time interval for temperature reading is decreased, using the standard method, the HiReTS total number increases, reaching a value 60 % bigger for the 15 s reading interval. Comparing the standard method with the linear extrapolation method, the use of a longer time period for the curve fitting results increases the HiReTS total number. This indicates that the temperature profiles at each measured point first increase at an increasing rate ($d^2T/dt^2 > 0$) and then curve downwards, ($d^2T/dt^2 < 0$) as the test time progresses. The cause for this is not well understood yet. Further testing is needed to determine the limit for the time interval for the linear extrapolation.

Table 4. HiReTS number for the fresh sample including the standard method and the extrapolations using linear regression.

	Time interval between temperature measurements		
Time interval used in the linear curve fitting	15 s	1 min	5 min
Standard Method	97	74	**61**
5 min	127	96	61
10 min	124	107	66
15 min	122	104	80
20 min	117	94	84

3.2.2 Aged Sample

The same jet fuel was allowed to age by recirculation at the heated HiReTS equipment during system upgrade, setup and tuning. During aging, the fuel sample reaches equilibrium with the atmospheric concentration of oxygen. As discussed above, this has the effect of increasing the tendency for thermal degradation. Figure 5 presents the temperature measured at the external surface of the test section for the aged sample. In this test, the blocking of the capillary tube by a solid particle caused a sudden temperature increase in the 75 min elapsed test time. The pressure increase reached 5.4 MPa, when the blockage was expelled. After that, the pressure fell back to 4.2 MPa and the temperature dropped back to its original path.

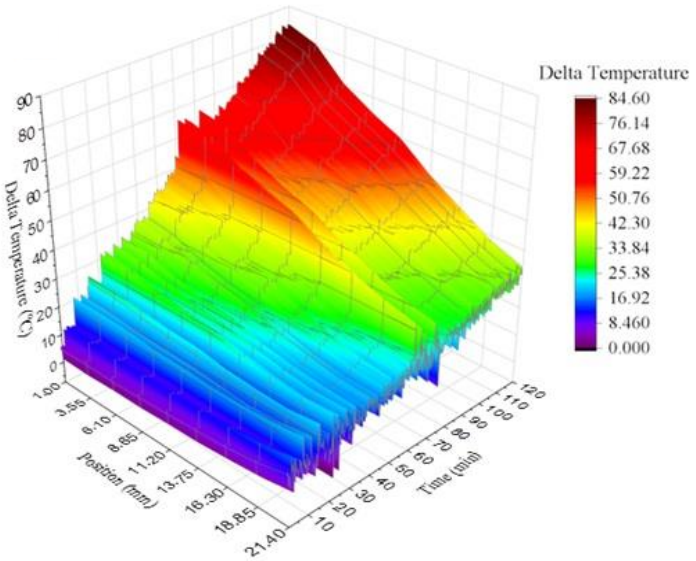

Figure 5. Temperature measured at the surface of the test section by the infrared camera during the HiReTS test of an aged fuel sample. The temperatures are displayed with a 15 seconds data acquisition interval.

Table 5 presents the HiReTS Number calculated for this experiment. The standard method provided a HiReTS total number of 438, which is indicative of a thermally stable fuel. However, the increase on thermal degradation when compared to the fresh fuel indicates the strong effect that the oxygen in solution has in the kinetics of the thermal degradation. Table 5 also presents the HiReTS total numbers obtained with the other methodologies. For this mixture with a stronger degradation rate, the results obtained from the other methods do not differ more than 17 % from the standard method. The measurements with 1 min interval increase the HiReTS number calculated by the standard method in about 9 % (470), while the measurements with the 15 s time interval increase in 17 % (506). The use of progressively longer periods for the linear curve fitting did not change the HiReTS number by more than 1 %, indicating that the temperature increase due to degradation for this sample has a rather linear behavior.

Table 5. HiReTS number for the aged sample including the standard method and the extrapolations using linear regression.

	Time interval between temperature measurements		
Time interval used in the linear curve fitting	15 s	1 min	5 min
Standard Method	506	470	**438**
5 min	513	472	438
10 min	509	476	436
15 min	508	469	436
20 min	510	473	440

4 CONCLUSIONS

In this work, the JFTOT and HiReTS methods were compared in terms of the basic characteristics of the flow and heat transfer in both methods. It is concluded that the JFTOT test subjects the fuel to a higher thermal stress than the HiReTS test, mostly due to the very long residence time under heating. However, this method has the drawback of having a complicated flow, affected by buoyancy and thermally developing conditions. The HiReTS method has a much simpler flow, a basically homogeneous turbulent flow, which tend to be statistically reproducible. Also, the evolution of the kinetics of degradation and deposition in the fuel would find a transport limited segregated flow in the JFTOT test section, while it would occur under a basically homogeneous flow in the HiReTS method, making it into a more statistically predictable test.

An original HiReTS equipment was retrofitted with new technologies and two kerosene samples were subjected to the HiReTS test, one fresh and the other aged, with the objective to compare different forms of calculating the HiReTS number under conditions of very high temperature oscillations. The temperature oscillations in the tests here were caused by an improper setting of the control system. It is concluded that the linear extrapolation method to calculate the HiReTS number is able to filter out temperature oscillations caused by measurement uncertainty and lack of proper temperature control and should be preferred over the standard method. Comparing the standard method with the linear extrapolation method, the use of a longer time period for the curve fitting resulted in an increase of the HiReTS total number. The effect was large for a sample with very large thermal stability, of the order of 30 %, and relatively smaller, of the order of 1 %, for a sample presenting higher degradation. The cause for this is not well understood yet. Further testing is needed to determine the limit for the time interval for the linear extrapolation.

5 ACKNOWLEDGEMENTS

Financial support for this work was provided by Petrobras. The authors gratefully acknowledge the comments by Dr. Anderson Rouge dos Santos, from Petrobras, to improve the presentation. The authors declare no competing financial interest.

6 REFERENCES

ASTM D1655-20e1, Standard Specification for Aviation Turbine Fuels, ASTM International, West Conshohocken, PA, 2020, www.astm.org.

ASTM D3241-20, 2014. “Standard Test Method for Thermal Oxidation Stability of Aviation turbine fuels”. ASTM International, West Conshohocken, PA, 2020, www.astm.org.

ASTM D6811-02, 2007. “Standard Test Method for Measurement of Thermal Stability of Aviation Turbine Fuels under Turbulent Flow Conditions (HiReTS Method)”. United States.

Beaver B., Gao L., Burgess-Clifford C., Sobkowiak M., 2005. “On the mechanisms of formation of thermal oxidative deposits in jet fuels. Are unified mechanisms possible for both storage and thermal oxidative deposit formation for middle distillate fuels?”. Energy & Fuels, Vol. 19, pp. 1574–1579.

Beaver, B.D., Kabana, C. and Schobert, H, 2009. Could jet fuel thermal oxidative degradation contributed to a recent commercial plane crash? A proposed hypothesis and experimental test plan. 11th International Conference on Stability, Handling and Use of Liquid Fuels 2009. 3. 1852-1872.

Bullock, S.P., Hobday, A., Lewis, C., 1998. “European Evaluation of JP8+100 Fuel and Its Impact on Engine/Fuel System Design”. Presented at the RTO AVT Symposium on Gas Turbine Engine Combustion, Emissions and Alternative Fuels, Lisbon, Portugal.

Dufferwiel, S., 2011. “Alternative Aviation Fuels – Aromatics & Thermal Stability”. E-Futures.

Ervin, J.S., Zabarnick, S., Williams, T.F., 2000, One-Dimensional Simulations of Jet Fuel Thermal-Oxidative Degradation and Deposit Formation Within Cylindrical Passages, J. Energy Resour. Technol. Dec 2000, 122(4): 229-238.

Giovanetti, A.J., Szetela, E.J., 1986. “Long-Term Deposit Formation in Aviation Turbine Fuel at Elevated Temperature”. Journal of Propulsion, Vol. 2, No. 5, pp. 450-456.

Heneghan, S.P, Zabarnick, S., Oxidation of jet fuels and the formation of deposit, Fuel, Volume 73, Issue 1, 1994, Pages 35-43.

Hazlett, R.N., 1991. “Thermal Oxidation Stability of Aviation Turbine Fuels”. American Society for Testing and Materials (ASTM): West Conshohocken, PA.

Huang, H., Spadaccini, L.J., Sobel, D.R., 2004. “Fuel-Cooled Thermal Management for Advanced Aeroengines”. J. Eng. Gas Turbines Power, Vol. 126, pp. 284−293.

Jankowski, A., 2010. “Heat Transfer in Combustion Chamber of Piston Engines”. Journal of KONES, Vol. 17, No. 1, pp. 187-197.

Jia, T., Gong, S., Pan, L., Deng, C., Zou, J.-J., Zhang, X., Impact of deep hydrogenation on jet fuel oxidation and deposition, Fuel, Volume 264, 2020, 116843.

Jiang, H., Ervin, J., West, Z., Zabarnick, S., 2013 “Turbulent Flow, Heat Transfer Deterioration, and Thermal Oxidation of Jet Fuel”. Journal of Thermophysics and Heat Transfer, Vol. 27, No. 4.

Kays, W.M., Crawford, M.E., 1993, Convective Heat and Mass Transfer, McGraw-Hill, 3rd Edition.

Kendall, D.R., Clark, R.H., Wolveridge, P.E., 1987, Fuels for Jet Engines: The Importance of Thermal Stability", Aircraft Engineering and Aerospace Technology, Vol. 59 No. 12, pp. 2-7.

Langton, R., Clark, C., Hewitt, M., Richards, L., 2010. “Aircraft Fuel Systems”; Encyclopedia of Aerospace Engineering. Wiley.

Morris, R.W., Jr., Miller, J., Limaye, S.Y., 2006. “Fuel Deoxygenation and Aircraft Thermal Management.” In 4th International Energy Conversion Engineering Conference and Exhibit (IECEC); American Institute of Aeronautics and Astronauts (AIAA): Reston, VA, pp 285−297.

Neageli, D.W., 1997. “Thermal Stability of Jet Fuels: Kinetics of Forming Deposit Precursors”. Southwest Research Institute: San Antonio, TX. NASA Contract NAG 3-1739.

NIST, 2018. “Welcome to the NIST WebBook”. National Institute of Standards and Technology. 23 July 2020 <https://webbook.nist.gov/>.

Panton, R., 2013, Incompressible Flow, Wiley, 4th Edition.

Pei, X., Hou, L., Ren, Z., 2015. “Flow Pattern Effects on the Oxidation Deposition Rate of Aviation Kerosene”. Energy Fuels, Vol. 29, pp. 6088-6094.

Sander, Z.H., West, Z.J., Ervin, J.S., Zabarnick, S., 2015. “Experimental and Modeling Studies of Heat Transfer, Fluid Dynamics, and Autoxidation Chemistry in the Jet Fuel Thermal Oxidation Tester (JFTOT)”. Energy & Fuels, Vol. 29, pp. 7036-7047.

Sarnecki, J., Gawron, B., 2017. “A Method of Assessing the Tendency of Aviation Fuels to Generate Thermal Degradation Products under the Influence of High Temperatures”. Journal of KONES, Vol. 24, No. 4.

Shah, R.K., London, A.L., 1978, Laminar Flow Forced Convection in Ducts - A Source Book for Compact Heat Exchanger Analytical Data, 1st Edition, Academic Press.

White, F., 2005, Viscous Fluid Flow, McGraw-Hill Education, 3rd. Edition.

Wilson, C.W., Blakey, S. e Spalton, T., 2010. “Quantitative Thermal Stability Testing”. The University of Sheffield and University of Leeds.

7 RESPONSIBILITY NOTICE

The authors are the only responsible for the printed material included in this paper.